GEOPHYSICAL RESEARCH LETTERS, VOL. 35, L20108, doi:10.1029/2008GL035813, 2008

Conservation of open solar magnetic flux and the floor in the heliospheric magnetic field

M. J. Owens,[1] N. U. Crooker,[2] N. A. Schwadron,[2] T. S. Horbury,[1] S. Yashiro,[3] H. Xie,[3] O. C. St. Cyr,[4] and N. Gopalswamy[4]

Received 26 August 2008; revised 25 September 2008; accepted 29 September 2008; published 30 October 2008.

[1] The near-Earth heliospheric magnetic field intensity, |**B**|, exhibits a strong solar cycle variation, but returns to the same "floor" value each solar minimum. The current minimum, however, has seen |**B**| drop below previous minima, bringing in to question the existence of a floor, or at the very least requiring a re-assessment of its value. In this study we assume heliospheric flux consists of a constant open flux component and a time-varying contribution from CMEs. In this scenario, the true floor is |**B**| with zero CME contribution. Using observed CME rates over the solar cycle, we estimate the "no-CME" |**B**| floor at ~4.0 ± 0.3 nT, lower than previous floor estimates and below |**B**| observed this solar minimum. We speculate that the drop in |**B**| observed this minimum may be due to a persistently lower CME rate than the previous minimum, though there are large uncertainties in the supporting observational data. **Citation:** Owens, M. J., N. U. Crooker, N. A. Schwadron, T. S. Horbury, S. Yashiro, H. Xie, O. C. St. Cyr, and N. Gopalswamy (2008), Conservation of open solar magnetic flux and the floor in the heliospheric magnetic field, *Geophys. Res. Lett.*, *35*, L20108, doi:10.1029/2008GL035813.

1. Introduction

[2] In situ observations of the heliospheric magnetic field intensity, |**B**|, over the last ~40 years show a strong solar cycle variation, with |**B**| varying in phase with sunspot number [e.g., *Richardson et al.*, 2002]. While the peak |**B**| varies considerably from cycle to cycle, each solar minimum has seen a return to a field intensity low of ~5 nT [e.g., *Richardson et al.*, 2002]. *Svalgaard and Cliver* [2005] recently developed an index based on geomagnetic activity which correlates strongly with |**B**|, and subsequently used it to infer |**B**| over the last ~130 years [*Svalgaard and Cliver*, 2007]. They reported the ~5 nT solar minimum |**B**| low has persisted during this time, and used a correlation between |**B**| and sunspot number to infer a "floor" in |**B**| at 1 AU of 4.6 nT, posited to occur for zero sunspot number. Observations of |**B**| for the current solar minimum, however, have dropped below 4.6 nT, bringing in to question the existence of a |**B**| floor, or at the very least requiring a re-assessment of its value. Using cosmic ray data, it has been suggested that a |**B**| floor can exist over multiple solar cycles but then suddenly change in value every ~50–100 years [*McCracken*, 2007], which is one possible explanation for the recent observations.

[3] A |**B**| floor implies the existence of a time-invariant component of the open solar flux. A number of authors [*McComas et al.*, 1992; *Webb and Howard*, 1994; *Owens and Crooker*, 2006, 2007] have suggested heliospheric magnetic flux consists of a constant open flux component, with a time-varying contribution from the closed flux carried by coronal mass ejections (CMEs), which provides the solar cycle variation in |**B**|. The return to the same value of |**B**| each solar minimum means flux added by CMEs must be balanced over the solar cycle, either by opening the closed flux via reconnection with open flux [interchange reconnection; *Crooker et al.*, 2002], or by disconnecting an equivalent amount of open flux [*McComas et al.*, 1992]. Using the observed CME rates and an estimate of the typical CME magnetic flux content, *Owens and Crooker* [2006] estimated that the observed solar cycle variability in |**B**| can be matched if CMEs contribute flux to the heliosphere for ~30–50 days.

[4] Constancy of open flux also features in a number of models of coronal and heliospheric solar cycle polarity reversal. *Fisk et al.* [1999] suggest that continual reconnection between open and closed flux at coronal hole boundaries allows the polarity reversal to proceed as a rotation of the heliospheric current sheet (HCS), conserving open flux throughout. *Fisk and Schwadron* [2001] propose that HCS rotation is driven by a diffusive process involving interchange reconnection. *Owens et al.* [2007] suggest the interchange reconnection occurs in the legs of CMEs, conserving but transporting open flux in the manner required for the polarity reversal.

[5] If, however, open flux disconnection does occur, and is at a pace independent of the flux added by CMEs, open flux need not be conserved, and a |**B**| floor is not required. Coronal inflows, which may be signatures of disconnection [*Wang et al.*, 1999] (though they could equally be signatures of interchange reconnection with the loop apex beyond the field of view [e.g., *Crooker et al.*, 2002]), exhibit a preference for solar longitudes where the HCS is orientated perpendicular to the solar equator [*Sheeley and Wang*, 2001]. Thus the reduction in |**B**| during the current solar minimum could be the result of the HCS being more warped than the previous minimum, and hence disconnecting a greater amount of open flux.

[6] In this study we estimate a new value for the |**B**| floor based on the assumption that the heliospheric magnetic field

[1]Space and Atmospheric Physics, The Blackett Laboratory, Imperial College London, London, UK.
[2]Center for Space Physics, Boston University, Boston, Massachusetts, USA.
[3]Department of Physics, Catholic University of America, Washington, D.C., USA.
[4]NASA Goddard Space Flight Center, Greenbelt, Maryland, USA.

0094-8276/08/2008GL035813$05.00

Table 1. The CME Rate Observations Used in This Study

Start Date	End Date	Source
20 Dec 1995	5 Jul 1998	Duty-cycle corrected CME rates from O. C. St. Cyr analysis of LASCO data [see *St. Cyr et al.*, 2000].
6 Jul 1998	11 Dec 2006	CME rates calculated from the LASCO CME catalog. Only events with radial widths >30 included. The data gap from Jun 1998 to Feb 1999 was excluded [see *Yashiro et al.*, 2004; *Gopalswamy et al.*, 2008]
12 Dec 2007	5 Jul 2008	Duty-cycle corrected CME rates from O. C. St. Cyr and H. Xie analysis of STEREO COR1 data. See http://cor1.gsfc.nasa.gov/catalog/

consists of a constant open flux component and a time-varying contribution from CMEs.

2. CME Rate Over the Solar Cycle

[7] Estimating the heliospheric flux contribution from CMEs requires a consistent set of CME-frequency (f) observations over the last solar cycle, in particular during the current and the previous solar minima. By "consistent", we mean that the same criteria are used to identify CMEs throughout the observations. The classification of CMEs in coronagraph data, however, is an inherently subjective process and will depend on the characteristics of the coronagraph used. Recently, there have been attempts to automate CME detection through the use of image processing techniques and algorithms [e.g., *Olmedo et al.*, 2008; *Robbrecht and Berghmans*, 2004]. While such methods are certainly more objective, it is currently unclear how well they separate CMEs from other coronal phenomenon [*Yashiro et al.*, 2008]. Thus an experienced human observer remains the best judge of what does and does not constitute a CME, and CME-rate data used in this study are restricted to human identification.

[8] The LASCO CME catalog [*Yashiro et al.*, 2004; *Gopalswamy et al.*, 2008], provides a regularly-updated list of CMEs identified in the LASCO data by human observers. Over the years, changes in observers will necessarily have led to different working definitions of a CME. In particular, since 2004 an increased interest in smaller-scale coronal transients has led to the inclusion of smaller events. Furthermore, CME rates derived from the CME catalog event list do not take instrumental duty cycle into account. Thus while the CME catalog provides an excellent resource for CME-based research, it is not immediately clear that is suited to the calculation of consistent CME rates over the solar cycle.

[9] *St. Cyr et al.* [2000] also compiled a catalog of LASCO CMEs during the previous solar minimum (12/1995 to 8/1998), with rates corrected for duty cycle. Duty cycle-corrected CME rates have also been calculated by the same observer (St. Cyr and, subsequently, Xie) during the current solar minimum (12/2006 to 6/2008) using the COR1 instrument on the STEREO spacecraft (see http://cor1.gsfc.nasa.gov/catalog/). Of course, no two coronagraphs will have the same optical performance characteristics, and this must be factored into the detectability of CMEs between instruments [e.g., *Webb and Howard*, 1994]. Where possible, St. Cyr and Xie performed an examination of the LASCO data for the COR1 CME detections, thus reducing the possibility of uneven counting techniques. In doing so, they have produced a consistent set of CME rates over the current and previous solar minima.

[10] A semi-consistent set of CME rates over the whole solar cycle can then be produced by supplementing the two sets of St. Cyr solar minimum rates with LASCO catalog-derived rates. This combination minimizes duty cycle effects, which, over the long time averages used in this study (at least a Carrington rotation), are of concern primarily at the start of the mission, covered by the corrected St. Cyr rates, and during the prolonged SOHO-outage from Jun 1998 to Feb 1999, which is removed. Furthermore, the effect of changing observers can be largely mitigated by excluding events with angular widths less than 30°. Table 1 summarizes the CME observations used in this study and Figure 1 (left) shows the resulting CME rate as a function of time. Blue, red and black crosses show data from St. Cyr's LASCO observations, the processed LASCO CME catalog and St. Cyr and Xie's STEREO observations, respectively. The black dashed line shows the LASCO CME catalog-derived rate, for CMEs with angular widths >30°. There is good agreement with the St. Cyr CME rates during both periods of overlap, suggesting a high level of consistency between all three sets of CME rates. Finally, note that while the lowest CME rates during the current (red) and the previous (blue) solar minimum are about the same ($\sim$0.4 day^{-1}), the CME rate during the present solar minimum is less variable and persistently lower. The error bars resulting from duty cycle, however, not shown for clarity, are particularly large during early 1996 (see Section 3).

3. Estimating the Heliospheric Magnetic Field Floor

[11] If the heliospheric field consists of a constant open flux and a time-varying CME contribution, there should be a strong relationship between CME frequency (f) and the magnetic field intensity in near-Earth space ($|\mathbf{B}|$). Figure 1 (middle) shows Carrington rotation (CR) averages of $|\mathbf{B}|$ as a function of f. National Space Science Center (OMNI) data are used for the $|\mathbf{B}|$ observations. Error bars are the standard errors on the mean for the 1-hour $|\mathbf{B}|$ used to construct the CR averages (most-probable CME rates are used, uncertainties from coronagraph duty cycle have not been included: See Section 4). Despite the considerable scatter, there is a clear trend between $|\mathbf{B}|$ and f, with a nearly linear relationship for $f \leq 3$ day^{-1}, after which the increase in $|\mathbf{B}|$ with f flattens off. In order to estimate the field intensity for no CMEs at the y-axis intercept, we fit a hyperbolic tangent function to the data, shown as the solid black curve. Dashed black curves show the 95% confidence interval. The fit matches the data well, with no systematic trends in the fit residuals. We find a no-CME value for $|\mathbf{B}|$ of 3.7 ± 0.7 nT. Figure 1 (right) shows the same data binned by CME frequency (0.25 day^{-1} bins are used, as this gives both sufficient sampling in CME rate and maintains a significant number of data points in each bin). Error bars are the standard errors on the mean of the CR averages. Here the trend becomes even more apparent, resulting in a floor of 4.0 ± 0.3 nT.

[12] From Figure 1 (middle) it is also apparent that for equivalent CME rates, $|\mathbf{B}|$ for the current solar minimum

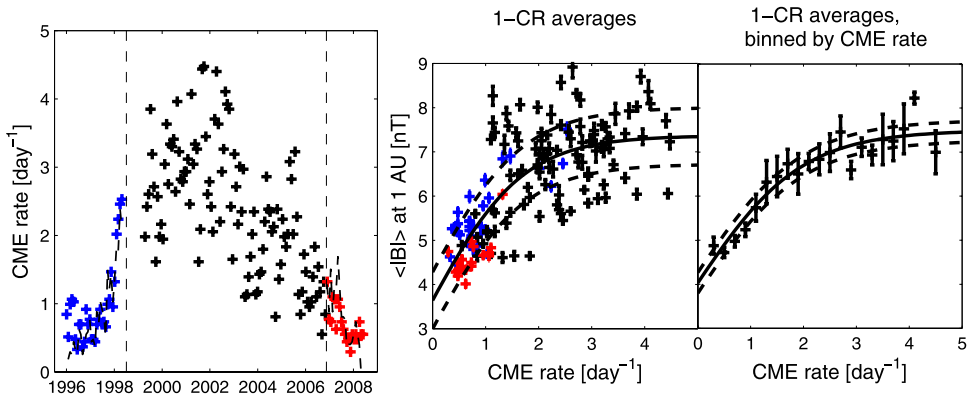

Figure 1. (left) Carrington rotation averages of CME frequency over the solar cycle. Blue, red and black crosses show data from St. Cyr's LASCO observations, the LASCO CME catalog and St. Cyr and Xie's STEREO observations, respectively. The black dashed line shows the LASCO CME catalog-derived CME rate, for CMEs with angular widths >30°. There is good agreement with the St. Cyr CME rates during both periods of overlap, suggesting a high level of consistency in the CME rates. (middle) Carrington rotation averaged CME frequencies as a function of 1-AU magnetic field intensities. (right) Same data as Figure 1 (middle) binned by CME frequency. Solid (dashed) black curves show the best hyperbolic tangent fits (95% confidence interval).

(red) is slightly lower than the previous cycle (blue). The large-scale trend between |**B**| and *f*, however, seems prevalent throughout the solar cycle.

4. Drop in |B| During the Current Minimum

[13] The Figure 2a shows 1- (6-) CR averages of |**B**| as a thin (thick) solid black line. The estimated no-CME |**B**| floor of 4.0 ± 0.3 nT is shown as the set of horizontal black lines. The present solar minimum (the red rectangle) has so far reached a 1- (6-) CR average |**B**| low of 4.1 (4.4) nT, while the previous minimum (the blue rectangle), reached a low of |**B**| = 4.6 (4.9) nT. Thus the observed value of $\Delta|\mathbf{B}|_{MIN}$, the change in the lowest field intensity between the current and previous solar cycle, is ∼0.5 nT.

[14] Figures 2c and 2d show the CME rates for the previous and current solar minima, with the most-probable values shown as open circles. Error bars are the result of

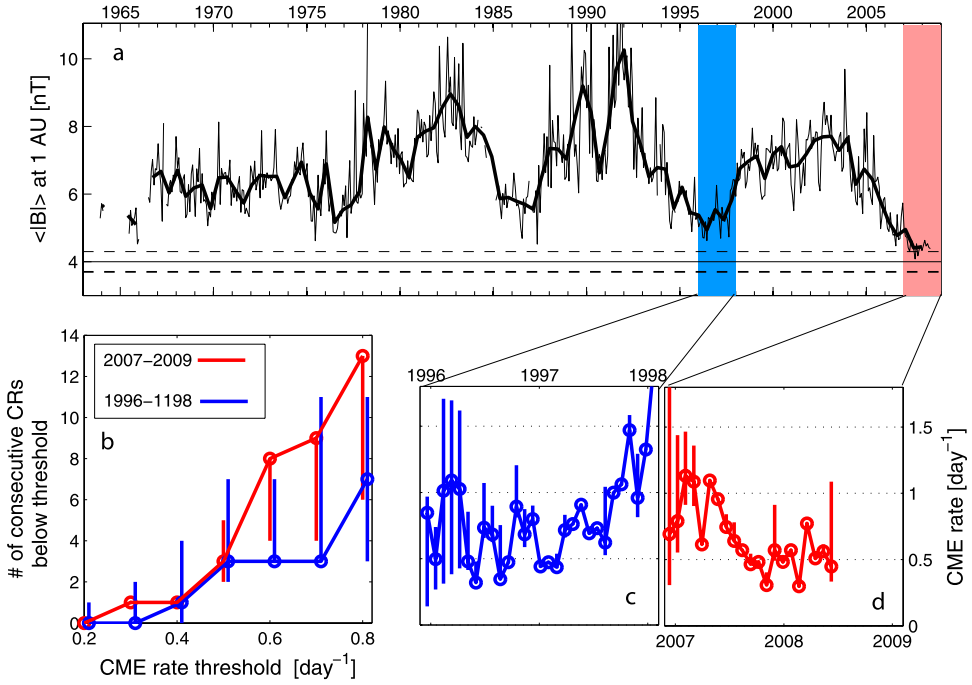

Figure 2. (a) The magnetic field intensity in near-Earth space since 1963. Thin (thick) lines show 1- (6-) CR averages. The horizontal black lines show the estimated |**B**| floor. (b) Maximum number of consecutive CRs for which the CME rate is below a certain threshold. Error bars are the result of coronagraph duty cycle. CME rates for the (c) previous and (d) current solar minima, with the most-probable values shown as open circles.

coronagraph duty cycle. The lowest 6- (12-) CR average CME rate is 0.51 ± 0.07 (0.56 ± 0.05) day^{-1} for the previous minimum, compared to 0.45 ± 0.05 (0.50 ± 0.04) day^{-1} for the current cycle. This drop in CME rates is not statistically significant. Figure 2b shows the maximum number of consecutive CRs for which the CME rate is below a certain threshold, with blue (red) lines indicating the previous (current) minimum. Error bars are again the result of coronagraph duty cycle. While the most-probable values, shown as open circles, suggest CME rates during the current minimum are persistently lower than the previous minimum, the large error bars mean this interpretation is speculative, at best. Furthermore, we cannot discount the possibility that the lowest CME activity from the previous solar minimum occurred before the first LASCO observations and is, therefore, not included in our data.

[15] Despite the uncertainties in the observed CME rates, we proceed using the most-probable values. To assess whether the observed drop in |**B**| can be explained in terms of CME rate, we use the model of *Owens and Crooker* [2006], in which a CME contributes ϕWb of flux to the heliosphere:

$$\phi = (1 - D)\phi_0 \exp[-\lambda t] \quad (1)$$

where D is the fraction of the CME flux which opens at launch (observed to be ~0.5 [e.g., *Owens and Crooker*, 2006]), ϕ_0 is the magnetic flux content of a typical CME, λ controls the time-scale (τ) over which the CME contributes flux to the heliosphere, and t is the time since CME eruption. The total CME contribution to the heliospheric field is then found by summing over all CMEs. Using CME rates from the LASCO CME catalogue and a value for ϕ_0 of 3×10^{12}Wb (the median force-free magnetic cloud estimate *Lynch et al.* [2005]), *Owens and Crooker* [2006] found the solar minimum-to-maximum variation in |**B**| was well matched by $\tau \sim 30-50$ days. This time scale is in agreement with the available suprathermal electron observations [*Owens and Crooker*, 2007].

[16] We have applied the *Owens and Crooker* [2006] model to the observed CME rates during the current and previous solar minimum to estimate $\Delta|\mathbf{B}|_{MIN}$ for a range of values of ϕ_0 and τ. We find that $\Delta|\mathbf{B}|_{MIN}$ ~0.5 nT requires higher values of ϕ_0 and/or τ than used by *Owens and Crooker* [2006]: For $\tau \sim 30-50$, the observed solar minimum CME rates require $\phi_0 \sim 1-2 \times 10^{13}$ to reproduce the observed $\Delta|\mathbf{B}|_{MIN}$. The value of $\phi_0 = 3 \times 10^{12}$Wb used by *Owens and Crooker* [2006] was based on force-free magnetic cloud fits, which have recently been shown to underestimate ϕ_0 by ~×5 [*Owens*, 2008], making $\phi_0 \sim 1-2 \times 10^{13}$Wb well within the observational constraints. Thus the lower |**B**| observed during the current minimum can potentially be explained in terms of the change in CME rates, for reasonable estimates of the free parameters. The long timescales for heliospheric flux balance mean the "time history" of the CME rate, not just the lowest value, determines the |**B**|.

5. Discussion

[17] We have used consistent CME rates from the current and previous solar minima, supplemented by solar maximum observations from the LASCO CME catalog, to construct a semi-consistent set of CME rates over the whole solar cycle. Carrington rotation averages of CME rate and magnetic field intensity in near-Earth space, |**B**|, show a strong correlation, with regression revealing a "no-CME" |**B**| floor of ~4.0 ± 0.3 nT. This is lower than the "no-sunspot" floor of 4.6 nT estimated using a correlation between sunspot number and geomagnetic indices [*Svalgaard and Cliver*, 2007]. Although sunspot number and CME frequency are generally well correlated [e.g., *Webb and Howard*, 1994], we suggest the small difference in floor values is due to not all CMEs originating at sunspot regions [*Gopalswamy et al.*, 2003]. *Owens and Crooker* [2006, 2007] estimated the non-CME component of the heliospheric field by comparing the change in |**B**| between solar minimum and maximum with the corresponding change in CME frequency. They reported a value ~4.5 nT, but their estimate of the magnetic flux content of a typical CME is likely to have been an underestimate, as discussed in Section 4. A higher CME magnetic flux content would yield a lower |**B**| floor, more in line with the findings in this study. Most importantly, our new "no-CME" estimate of the |**B**| floor is in agreement with observations from the current solar minimum. While this certainly does not prove the existence of a |**B**| floor, we argue that the observations during the current solar minimum do not disprove the idea that there is a constant heliospheric flux component.

[18] On the basis of quantitative modeling results, we propose that the lower |**B**| observed during the current solar minimum may be the result of a persistently lower CME rate than the previous minimum. We note, however, that large uncertainties in the supporting observational data, resulting from both duty-cycle effects and longer-term data-coverage issues, make this conclusion speculative at best. With the observational caveats in mind, we modeled the most-probable CME rates. While a more complete exploration of the model parameter space is required, for timescales of CME flux contribution (τ) similar to those previously proposed [*Owens and Crooker*, 2006, 2007], the difference in |**B**| between the current and previous minima requires a higher value for the typical CME magnetic flux (ϕ_0). This higher value of ϕ_0 is in good agreement with recent findings [*Owens*, 2008], as well as the lower floor suggested by this study. If ϕ_0 and τ are constant over the solar cycle, however, the extra CME magnetic flux would result in an overestimate in |**B**| at solar maximum. Thus a constant |**B**| floor requires the heliospheric flux contribution from a typical CME to be less at solar maximum than at solar minimum, in agreement with the observed flattening of |**B**| with f for $f \geq 3\text{day}^{-1}$ in Figure 1. This can be achieved by either ϕ_0 and/or τ varying over the solar cycle. A drop in ϕ_0 could be associated with a solar maximum increase in the fraction of smaller CMEs or the observed solar maximum decrease in the fraction of magnetic cloud CMEs [e.g., *Riley et al.*, 2006], while a decrease in τ could result from the increased complexity in the solar maximum coronal magnetic field allowing CME flux to reconnect faster than at solar minimum. Clearly, this subject merits further study.

[19] **Acknowledgments.** This research was funded by the STFC (UK). NC was supported by NSF grant ATM-0553397. Work at BU was

also supported by CISM which is funded by the National Science Foundation STC program under Agreement ATM-012950.

References

Crooker, N. U., J. T. Gosling, and S. W. Kahler (2002), Reducing heliospheric magnetic flux from coronal mass ejections without disconnection, *J. Geophys. Res.*, *107*(A2), 1028, doi:10.1029/2001JA000236.

Fisk, L. A., and N. A. Schwadron (2001), The behaviour of the open magnetic field of the Sun, *Astrophys. J.*, *560*, 425–438.

Fisk, L. A., T. H. Zurbuchen, and N. A. Schwadron (1999), Coronal hole boundaries and their interaction with adjacent regions, *Space Sci. Rev.*, *87*, 43–54.

Gopalswamy, N., A. Lara, S. Yashiro, S. Nunes, and R. A. Howard (2003), Coronal mass ejection activity during solar cycle 23, in *Solar Variability as an Input to the Earth's Environment*, edited by A. Wilson, Eur. Space Agency Spec. Publ., ESA-SP 535, 403–414.

Gopalswamy, N., S. Yashiro, G. Michalek, G. Stenborg, A. Vourlidas, S. Freeland, and R. Howard (2008), The SOHO/LASCO CME catalog, *Earth Moon Planets*, in press.

Lynch, B. J., J. R. Gruesbeck, T. H. Zurbuchen, and S. K. Antiochos (2005), Solar cycle-dependent helicity transport by magnetic clouds, *J. Geophys. Res.*, *110*, A08107, doi:10.1029/2005JA011137.

McComas, D. J., J. T. Gosling, and J. L. Phillips (1992), Interplanetary magnetic flux: Measurement and balance, *J. Geophys. Res.*, *97*, 171–177.

McCracken, K. G. (2007), Heliomagnetic field near Earth, 1428–2005, *J. Geophys. Res.*, *112*, A09106, doi:10.1029/2006JA012119.

Olmedo, O., J. Zhang, H. Wechsler, A. Poland, and K. Borne (2008), Automatic detection and tracking of coronal mass ejections in coronagraph time series, *Sol. Phys.*, *248*, 485–499.

Owens, M. J. (2008), Combining remote and in situ observations of coronal mass ejections to better constrain magnetic cloud reconstruction, *J. Geophys. Res.*, doi:10.1029/2008JA013589, in press.

Owens, M. J., and N. U. Crooker (2006), Coronal mass ejections and magnetic flux buildup in the heliosphere, *J. Geophys. Res.*, *111*, A10104, doi:10.1029/2006JA011641.

Owens, M. J., and N. U. Crooker (2007), Reconciling the electron counterstreaming and dropout occurrence rates with the heliospheric flux budget, *J. Geophys. Res.*, *112*, A06106, doi:10.1029/2006JA012159.

Owens, M. J., N. A. Schwadron, N. U. Crooker, W. J. Hughes, and H. E. Spence (2007), Role of coronal mass ejections in the heliospheric Hale cycle, *Geophys. Res. Lett.*, *34*, L06104, doi:10.1029/2006GL028795.

Richardson, I. G., H. V. Cane, and E. W. Cliver (2002), Sources of geomagnetic activity during nearly three solar cycles (1972–2000), *J. Geophys. Res.*, *107*(A8), 1187, doi:10.1029/2001JA000504.

Riley, P., C. Schatzman, H. V. Cane, I. G. Richardson, and N. Gopalswamy (2006), On the rates of coronal mass ejections: Remote solar and in situ observations, *Astrophys. J.*, *647*, 648–653.

Robbrecht, E., and D. Berghmans (2004), Automated recognition of coronal mass ejections (CMEs) in near-real-time data, *Astron. Astrophys.*, *425, 1097–1106.*

Sheeley, N. R., Jr., and Y.-M. Wang (2001), Coronal inflows and sector magnetism, *Astrophys. J. Lett.*, *562*, L107–L110.

St. Cyr, O. C., et al. (2000), Properties of coronal mass ejections: SOHO LASCO observations from January 1996 to June 1998, *J. Geophys. Res.*, *105*, 18,169–18,185.

Svalgaard, L., and E. W. Cliver (2005), The IDV index: Its derivation and use in inferring long-term variations of the interplanetary magnetic field strength, *J. Geophys. Res.*, *110*, A12103, doi:10.1029/2005JA011203.

Svalgaard, L., and E. W. Cliver (2007), A floor in the solar wind magnetic field, *Astrophys. J. Lett.*, *661*, L203–L206.

Wang, Y.-M., N. R. Sheeley Jr., R. A. Howard, N. B. Rich, and P. L. Lamy (1999), Streamer disconnection events observed with the LASCO coronagraph, *Geophys. Res. Lett.*, *26*, 1349–1352.

Webb, D. F., and R. A. Howard (1994), Solar cycle variation of coronal mass ejections and the solar wind mass flux, *J. Geophys. Res.*, *99*, 4201–4220.

Yashiro, S., N. Gopalswamy, G. Michalek, O. C. St. Cyr, S. P. Plunkett, N. B. Rich, and R. A. Howard (2004), A catalog of white light coronal mass ejections observed by the SOHO spacecraft, *J. Geophys. Res.*, *109*, A07105, doi:10.1029/2003JA010282.

Yashiro, S., G. Michalek, and N. Gopalswamy (2008), A comparison of coronal mass ejections identified by manual and automatic methods, *Ann. Geophys. J.*, *26*, 3103–3112.

N. U. Crooker and N. A. Schwadron, Center for Space Physics, Boston University, 725 Commonwealth Avenue, Boston, MA 02215, USA.

N. Gopalswamy, NASA Goddard Space Flight Center, Mail Code 671, Greenbelt, MD 20771, USA.

T. S. Horbury and M. J. Owens, Space and Atmospheric Physics, The Blackett Laboratory, Imperial College London, London SW7 2AZ, UK. (m.owens@imperial.ac.uk)

O. C. St. Cyr, NASA Goddard Space Flight Center, Mail Code 695, Greenbelt, MD 20771, USA.

H. Xie and S. Yashiro, Department of Physics, Catholic University of America, 620 Michigan Avenue, Washington, DC 20064, USA.